Neuroimmune guidance cues in vascular (patho)physiology

Vreeken, D.

Chapter 4

Eph receptor B2 stimulates human monocyte adhesion and migration independently of it EphrinB ligands

Dianne Vreeken[1]
Caroline Suzanne Bruikman[1]
Stefan Martinus Leonardus Cox
Huayu Zhang
Reshma Lalai
Angela Koudijs
Anton Jan van Zonneveld
Gerard Kornelis Hovingh
Janine Maria van Gils

[1] Authors contributed equally to this paper
Journal of Leukocyte Biology. 2020 Sep;108(3)

Abstract

The molecular basis of atherosclerosis is not fully understood and mice studies have shown that Ephrins and EPH receptors play a role in the atherosclerotic process. We set out to assess the role for monocytic EPHB2 and its Ephrin ligands in human atherosclerosis and show a role for EPHB2 in monocyte functions independently of its EphrinB ligands. Immunohistochemical staining of human aortic sections at different stages of atherosclerosis showed that EPHB2 and its ligand EphrinB are expressed in atherosclerotic plaques and that expression proportionally increases with plaque severity. Functionally, stimulation with EPHB2 did not affect endothelial barrier function, nor did stimulation with EphrinB1 or EphrinB2 affect monocyte-endothelial interactions. In contrast, reduced expression of EPHB2 in monocytes resulted in decreased monocyte adhesion to endothelial cells and a decrease in monocyte transmigration, mediated by an altered morphology and a decreased ability to phosphorylate FAK. Our results suggest that EPHB2 expression in monocytes results in monocyte accumulation by virtue of an increase of transendothelial migration, which can subsequently contribute to atherosclerotic plaque progression.

Graphical abstract

EPHB2 expression in monocytes promotes monocyte accumulation by increasing monocyte adhesion and transendothelial migration; subsequently, this can contribute to atherosclerotic plaque progression.

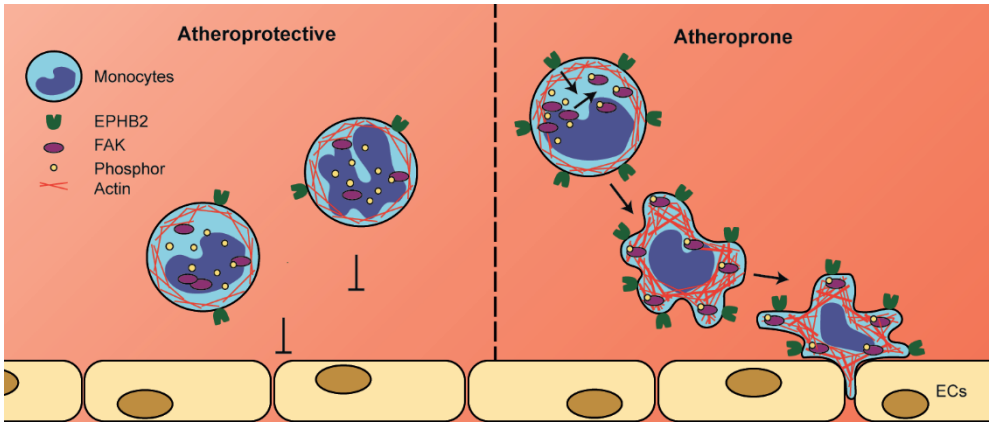

1. Introduction

Cardiovascular disease (CVD), caused by atherosclerosis, remains the leading cause of death (1). Despite the use of CVD risk lowering agents patients still suffer from CVD events, which suggest that additional, hitherto unaddressed, factors are involved (2, 3). Recently, a long-assumed role for inflammation in the atherosclerotic process has been proven (4-6), indicating that other pathophysiologic processes may play a role in CVD development. Unraveling novel players in the complex atherosclerotic process may ultimately result in novel targets for therapies to address the endemic burden of atherosclerosis.

Neuroimmune guidance cues (NGCs) are a group of proteins, consisting of four families of guidance molecules and their receptors, Netrins, Slits, Ephrins and Semaphorins. These cues were originally found to play a crucial role in the process of axon growth. However, NGCs have also been shown to play a role in atherosclerosis, as NGCs also regulate the development of the vascular system, maintain the physiological function of endothelial cells and play an important role in immune cell trafficking (7-9). The endothelial expression of several NGCs has been shown to differ between athero-resistant and athero-prone aortic regions. Moreover, NGCs have been implicated in leukocyte adhesion and migration, which implies that NGCs are crucial in the initial step of atherogenesis (10). Specifically, several studies have shown that members of the Ephrin family are involved in atherosclerosis related processes (10-15).

Erythropoietin-producing hepatocellular receptors (EPHs) and their EPH receptor interacting protein (Ephrin) ligands comprise a large family of receptor tyrosine kinases with 14 EPH receptors and 8 Ephrin ligands that are both membrane bound. A special feature of the Ephrins and their receptors is that they can induce bidirectional signaling. Not only does binding of the ligand to the receptor induce signaling (forward signaling), but also receptor-to-ligand binding induces signaling (reverse signaling). Both forward and reverse Ephrin signaling impacts on a variety of signaling pathways that mostly converge to regulation of the cytoskeleton and therewith can influence processes such as cellular adhesion, migration and vascular stability. Due to its role in a variety of cellular processes, deregulation of the Ephrins have been associated with several diseases, including atherosclerosis (16).

Multiple Ephrins and EPH receptors have been found in human atherosclerotic plaques (13, 14, 17). In addition the EPH receptor genes *EPHA2*, *EPHA8* and *EPHB2* are located on chromosome 1 within region *1p34-36,* which has been identified as a locus for myocardial infarction by a genome wide search for susceptibility genes for myocardial infarction (18). However, the functional role for Ephrins and EPH receptors in atherosclerosis is largely unexplored. We hypothesized that these molecules are expressed in human monocytes

and endothelial cells, both culprit cell types in atherosclerosis, and contribute to atherogenesis. In this study we identified the EPHB2 receptor and the ligands EphrinB1 and EphrinB2 as highly expressed Ephrin family members on monocytes and endothelial cells respectively. In addition, we showed increasing expression of both EPHB2 and EphrinB in progressing stages of atherosclerosis. Furthermore, we demonstrated an important EphrinB ligand-independent role for EPHB2 in the atherosclerotic process, by promoting monocyte adhesion through phosphorylation of focal adhesion kinases (FAK).

2. Materials and methods

2.1 Database

We evaluated which NGCs are expressed by either monocytes or endothelial cells by means of the GENEVESTIGATOR (19) software. All published data on the Affymetrix Human Genome U133 Plus 2.0 Array (HG0U133 Plus 2.0/GPL570) platform on human leukocyte, endothelial cell or vascular smooth muscle cell gene expression were extracted and analyzed for Ephrin ligands and EPH receptor expression.

2.2 Immunohistochemistry/fluorescence of human tissue sections

The expression profiles of EPHB2 and EphrinB in human abdominal aortas at different stages of atherosclerosis were analyzed. The abdominal aorta segments used for this study were harvested during renal surgery. Use of this material is approved by the Medical and Ethical Committee of the Leiden University Medical Center (Leiden, the Netherlands). Approximately 3 cm of arterial material was fixed with formaldehyde and subsequently decalcified with Kristensen's solution to allow sectioning. The tissue was sliced in 5-mm segments and paraffin embedded. Tissue sections of 4-µm were prepared from each segment and each tissue block was classified for atherosclerotic stage using the revised classification of the American Heart Association (20). In sections with multiple lesions, grading was dictated by the most advanced lesion present.

Before staining, the slides were deparaffinized in 100% xylene and rehydrated in ethanol. Heat-induced epitope retrieval was performed in citrate buffer (pH 6.0) for 20 min at 98°C. Next, non-specific antigens were blocked with 1% bovine serum albumin (BSA) in Tris-buffered saline (TBS) for 30 minutes, followed by incubation with goat-anti-EPHB2 (5 µg/ml, AF467, R&D Systems, Minneapolis, MN, USA) or mouse-anti-EphrinB (1.5 µg/ml, 37-8100, Thermofisher, Rockford, IL, USA) for 60 minutes. Slides were incubated with horseradish peroxidase (HRP)-labelled rabbit-anti-goat (1:2000, P0160, Dako, Glostrup, Denmark) or HRP-labelled goat-anti-mouse (1:80, P0447, Dako, Glostrup, Denmark) secondary antibody for 60 minutes and counterstained with

NovaRed Peroxidase (SK-4800, Vector laboratories, Burlingame, CA, USA). Slides were covered with glycergel (C0563, Agilent, Glostrup, Denmark) or pertex (00801, Histolab, Västra Frölunda, Sweden) and a glass coverslip. For double staining slides were incubated overnight with goat-anti-EPHB2 together with either mouse-anti-CD68 (1:100, MCA1815T, BioRad, Temse, Belgium) or mouse-anti-CD45 (1:100, MBS245401, MyBioSource, San Diego, CA, USA). After a 30-minute incubation with the secondary antibodies alexa568-labelled donkey-anti-goat and alexa488-labelled donkey-anti-mouse (1:250, A11057 and A21202, Invitrogen Molecular probes, Eugene, OR, USA) slides were mounted with ProLong™ Gold Antifade mountant with DAPI (P36931, Thermo Fisher, Eugene, OR, USA).
Images were taken with the Pannoramic MIDI slide scanner and processed and quantified with HistoQuant software from 3DHistech. The investigator performing and scoring the grade of staining was blinded for the stage of atherosclerosis.

2.3 Primary cells, cell lines and media

2.3.1 Human umbilical vein endothelial cell isolation

Primary human umbilical vein endothelial cells (HUVECs) were isolated from human umbilical cords obtained at the Leiden University Medical Center after written informed consent and ensuring that collection and processing of the umbilical cord was performed anonymously. The umbilical vein was flushed with phosphate-buffered saline (PBS), using glass cannulas, to remove all remaining blood. Endothelial cells were detached by infusion of the vein with Trypsin/EDTA (1x) (BE02-007E, Lonza, Verviers, Belgium) solution and incubation at 37°C for 15 minutes. After incubation the cell suspension was collected and taken up in endothelial cell growth medium (EGM2 medium, C222111 supplemented with C39211, Promocell, Heidelberg, Germany) with 1% antibiotics. After flushing the umbilical vein once more with PBS, to ensure all detached cells are collected, cells were pelleted by centrifugation at 1200rpm for 7 minutes. The cell pellet was dissolved in fresh EGM2 medium and cells were cultured on gelatin (1%) coated surfaces.

2.3.2 THP1 cells

THP1 (TIB-202, ATCC, Middlesex, UK) were cultured in RPMI 1640 medium (22409, Gibco, Paisley, UK) supplemented with 10% fetal calf serum (FCS), 1% L-glutamine, 1% antibiotics (penicillin/streptomycin, 15070063, Gibco, Paisley, UK) and 25 nM β-mercaptoethanol. Differentiation of THP1 cells was achieved by a 3-day incubation with 100 nM phorbol 12-myristate-13-acetate (PMA) after which cells were cultured for another 5 days in normal growth medium.

2.3.3 CD14+ Peripheral blood mononuclear cells

Peripheral blood mononuclear cells (PBMCs) were isolated from buffy coats (Ethical Approval Number BTL 10.090) obtained after informed written consent by density gradient separation using Ficoll. CD14 Microbeads (130-050-201, Miltenyi Biotec, Bergisch Gladbach, Germany) and LS columns (130-042-401, Miltenyi Biotec, Bergisch Gladbach, Germany) were used for magnetic separation of CD14 positive monocytes. Isolated cells were kept in RPMI 1640 medium supplemented with 10% FCS, 1% L-glutamine and 1% antibiotics (penicillin/streptomycin). Cells were stimulated with 20 ng/ml macrophage colony-stimulating factor (130-093-963, Miltenyi Biotec, Bergisch Gladbach, Germany) for 7 days to induce monocyte-to-macrophage differentiation.

2.4 Transduction of THP1 cells

To achieve a knockdown of EPHB2 or EphrinB1, THP1 monocytes were transduced with lentiviral particles encoding shRNA against de coding region of EPHB2 or EphrinB1 (MISSION library Sigma-Aldrich, TRCN0000006424 or TRCN0000058656 respectively) or a mock. Selection of transduced cells was achieved using puromycin (3.33 µg/ml).

2.5 Barrier function assay

Endothelial barrier function analysis was performed with impedance-based cell monitoring using the electric cell-substrate impedance sensing system (ECIS Zθ, Applied Biophysics). ECIS plates (96W20idf PET, Applied Biophysics, Troy, NY) were pretreated with 10 mM L-Cystein and coated with 1% gelatin. Baseline resistance was measured over approximately 1 hour after which endothelial cells were added to the plate. Multiple frequency/time mode was used for the real-time assessment of the barrier and monolayer confluence. After approximately 24 hours when a stable barrier was formed, endothelial cells were stimulated with 500 ng/ml of recombinant EPHB2 (5189-B2, R&D Systems, Minneapolis, MN, USA).

2.6 Adhesion assay

THP1 cells with or without knockdown were labelled with 5 µg/ml Calcein AM (C3100MP, Molecular Probes, Eugene, OR, USA) and incubated on top of a monolayer of HUVECs for 30 min at 37°C. Non-adhering cells were washed away by multiple washing steps with PBS after which the cells were lysed in Triton-X 0.5% for 10 minutes. Fluorescence was measured at λex 485nm and λem 514nm. Each condition was performed in triplicate. In case of cell stimulation, THP1 cells were stimulated with 500 ng/ml recombinant EphrinB1 (7654-EB, R&D Systems, Minneapolis, MN, USA) or

EphrinB2 (7397-EB, R&D Systems, Minneapolis, MN, USA) for 30 minutes before addition to the monolayer of endothelial cells.

2.7 Migration assay

Chemotaxis of THP1 monocytes was measured using a 24-well Boyden chamber with a 5 µm pore size filter (734-1573, Corning, Kennebunk, ME, USA) coated with 10 µg/ml Fibronectin (F4759, Sigma, Saint Louis, MO, USA). Cell migration towards 10 ng/ml recombinant human monocyte chemotactic protein (MCP-1; 279-MC, R&D Systems, Minneapolis, MN, USA) and/or 500 ng/ml EphrinB1 or EphrinB2 was measured after 3 hours. Cells were resuspended and counted in randomly selected fields for each well to determine the number of cells that had migrated into the lower chamber. Each condition was performed in triplicate.

2.8 Real-time PCR

Total RNA was isolated using TRIzol and the RNeasy Mini Kit (74106, Qiagen, Hilden, Germany) according to manufacturer's instructions. Total RNA was reverse transcribed using M-MLV Reverse Transcriptase Kit (M1701, Promega, Madison, WI, USA). RT-PCR analysis was conducted using SYBR Select Master Mix (4472908, Applied Biosystems, Vilnius, Lithuania) and the forward and reverse primers as indicated in Supplemental table 1. The PCR cycling conditions were: Initial denaturation at 95°C for 10 minutes, followed by 40 cycles at 95°C for 15 seconds, 60°C for 30 seconds and 72°C for 30 seconds, followed by a final extension step at 72°C for 10 minutes. mRNA expression was normalized to expression of GAPDH and expressed as fold change compared to untreated.

2.9 Immunoblot analysis

THP1 cells were washed with cold PBS and lysed in cold RIPA buffer (9806, Cell signaling, Danvers, MA, USA). After centrifugation of the samples at 14000rpm for 10 minutes at 4 °C, protein concentration in the supernatant was measured using the Pierce BCA Protein Assay Kit (23255, Thermo Scientific, Rockford, IL, USA). Equal amounts of protein sample were denatured using DTT and heating at 95°C for 10 minutes followed by size separation on a 10% Mini-PROTEAN gel (4561033, Biorad, Temse, Belgium). Proteins were transferred to PVDF membranes (1704156, Biorad, Temse, Belgium) using the Trans-Blot Turbo system (Biorad) after which membranes were blocked in either TBST-5% BSA (A2058, Sigma, Saint Louis, MO, USA) for phosphorylated proteins or TBST-5% milk. Overnight incubation was performed with primary antibodies against EPHB2 (0,5µg/ml, AF467, R&D systems, Minneapolis, MN,

USA), EphrinB (1:250, 37-8100, ThermoFisher, Eugene, OR, USA) p38 (1:1000, 9211, Cell signaling, Danvers, MA, USA), p-p38 (1:1000, 9212, Cell signaling), p42 (1:1000, 9102, Cell signaling), P-p42 (1:1000, 4376, Cell signaling), FAK (1:500, 3283, Cell signaling), P-Y397 FAK (1:500, 3283, Cell signaling), P-Y925 FAK (1:500, 3284, Cell signaling), Akt (1:1000, 4060, Cell signaling), P-Akt (1:1000, 4691, Cell signaling) or GAPDH (1:5000, 5174S, Cell signaling). Incubation with HRP-conjugated secondary antibodies (1:5000, Dako, Glostrup, Denmark) and Western lightning ECL (NEL103001EA, PerkinElmer, Waltham, MA, USA) or SuperSignal Western Blot Enhancer (46640, ThermoFisher, Rockford, IL, USA) enabled us to visualize protein bands with the ChemiDoc Touch Imaging System (Biorad). Expression was quantified using ImageLab software (Biorad) and ImageJ software (http://rsbweb.nih.gov/ij/).

2.10 Immunofluorescence of cultured cells

Monocytes were incubated on fibronectin-coated (10 µg/ml, F4759, Sigma, Saint Louis, MO, USA) flat bottom 96-wells plates for 30 minutes, washed with PBS, fixed with 4% paraformaldehyde in Hanks' Balanced Salt Solution modified with calcium and magnesium (HBSS++) for 10 minutes and permeabilized with 0.1% Triton X-100 for 1 minute. After a 30-minute blocking step with 2% Casein in HBSS++, wells were incubated with Phalloidin-Rhodamine (1:200, P1951, Sigma, Saint Louis, MO, USA) for 1h. Excess Phalloidin staining was washed off and cells were imaged using the ImageXpress (Molecular Devices) and cell area was quantified using MetaXpress (Molecular Devices).

2.11 Statistical analyses

Data was analyzed by unpaired two-tailed t-tests for two groups or with ANOVA and post-hoc t-tests by the Tukey method for multiple groups. P-values of <0.05 were considered statistically significant. All statistical analyses were performed with SPSS version 24 or Graphpad Prism 7.

3. Results

3.1 Increased expression of EPHB2 and EphrinB in progressive human atherosclerotic lesions

Atherosclerosis is a systemic inflammatory disease, characterized by the accumulation of inflammatory cells in the vascular wall (21). Monocyte derived macrophages are key players in the lesion development (22). Therefore, we investigated the expression of Ephrin ligands and receptors in human monocytes and in atherosclerotic lesions. For this we combined published data within the Affymetrix Human Genome U133 Plus 2.0

Array platform and determined the specific Ephrins and EPH receptors expressed by leukocytes relative to the averaged normalized expression (Fig. 1A). In general, all ephrin ligands were expressed moderately in human leukocytes, with the highest expression observed for *EphrinA1*, *EphrinA3*, *EphrinA4* and *EphrinB1*. Expression of Ephrins differed minimally between leukocytes. In addition, the EPH receptors *EPHA1*, *EPHA2*, *EPHA8*, *EPHA10*, *EPHB2*, *EPHB3*, *EPHB4* and *EPHB6* were moderately expressed in all leukocytes. Strikingly, *EPHA1* and *EPHA4* were more abundant in lymphocytes, while *EPHB2* was more abundantly expressed in human monocytes and macrophages. Based on this observation, an observed increase in *EPHB2* expression upon monocyte-to-macrophage differentiation (Supplemental fig. 1) and combined with the fact that the *EPHB2* gene is located on a myocardial infarction susceptibility locus (18), we hypothesized a role for monocytic EPHB2 in atherosclerosis development. To investigate this, immunohistochemical staining for EPHB2 was performed on 24 aortic specimens with varying stages of atherosclerosis, ranging from Stage I (Normal, Adaptive Intimal Thickening, Intima Xantoma) to Stage IV (Healing Rupture, Fibrous Calcifies Plaque). EPHB2 was near absent in normal vascular tissue (Fig. 1B and C stage I). However, expression was found to progressively increase with atherosclerotic lesion formation, up to a 17-fold increase in stage IV (Fig. 1B and C). As EPHB2 expression was primarily observed in severe atherosclerotic lesions we performed a double staining of EPHB2 with the leukocyte marker cluster of differentiation (CD)45 or the monocyte/macrophage marker CD68 on Stage IV tissue sections to determine the contribution of immune cells to the observed increase in EPHB2 expression. Double staining with CD45 showed that around 25% of the CD45 positive area was also positive for EPHB2 (Supplemental fig. 2). Double staining of EPHB2 with CD68 revealed that around half of the area occupied by CD68+ cells was double positive for EPHB2 (Fig. 1D and E). Moreover, approximately 80% of the EPHB2+ area was also positive for CD68, together indicating that most cells positive for EPHB2 were monocytes/macrophages.

It is well established that the recruitment and accumulation of monocytes is regulated by both chemoattractant signals and changes in the adhesive properties of the endothelium lining the vascular wall (21). Since we suspected an interaction of monocytic EPHB2 with Ephrin ligands expressed by the endothelial lining of the vessel wall, the expression of Ephrin ligands in endothelial cells was determined. Again, publicly available data were combined and showed that endothelial cells highly expressed all Ephrin ligands except *EphrinA2*, which is only moderately expressed. Most highly expressed were the ligands *EphrinA1* and *EphrinB2* (Fig. 2A). Since the EPHB2 receptor has the highest binding affinity for the ligands EphrinB1 and EphrinB2 (23) and an increase in endothelial mRNA expression of *EphrinB1* was observed when cells were

exposed to pro-atherosclerotic conditions (Fig. 2B), the atherosclerotic lesions were also stained for EphrinB ligands. We observed EphrinB expression in normal aortic tissue without atherosclerotic plaques (Fig. 2B and C stage I). When plaques at different stages were present, the expression of EphrinB remained relatively constant. However, at the stage of a calcified fibrous plaque, the expression of EphrinB increased (1.6-fold, Fig. 2C and D stage IV). As EphrinB expression was not specific for endothelial cells and EphrinB ligands were also expressed in leukocytes and vascular smooth muscle cells (Fig. 1A and 2A), a region specific quantification was performed to explore the expression in the different cell types within the plaques. The increase in EphrinB expression was mainly observed in the intima and primarily in the most severe disease state (Fig. 2E). In addition, when looking specifically to the plaque area an increase in EphrinB expression was observed (Fig. 2F).

Figure 1 Increased expression of EPHB2 in progressive human atherosclerotic lesions. (A) Expression heatmap of Ephrin family ligands and their receptors in human leukocytes. Blue indicates lower and red higher expression. (B) Overview pictures of immunohistochemical staining for EPHB2 in human aortic sections in different stages of atherosclerosis. Lower images show higher-power magnification of the arrow-indicated fields. Scale bars represent 350 and 50 µM respectively. (C) Quantification of EPHB2 signal. Results are relative to stage I, set as 1. Mean ± s.e.m. of n=6. *P < 0.05. (B-C) Stage *I*; Normal, Adaptive Intimal Thickening, Intima Xantoma, *II*; Pathologic Intimal Thickening, Early Fibroatheroma, *III*; Late fibroatheroma, Thin Cap Fibroatheroma, Ruptured Plaque, *IV*; Healing Rupture, Fibrous Calcifies Plaque. (D) Overview and zoom-in pictures of immunofluorescent staining for EPHB2 (red), CD68 (green) and nuclei (blue) in stage IV human aortic sections. Scale bars represent 300 and 25 µm respectively. (E) Quantification of fluorescent signal in plaque shoulder regions. Results are quantified as positive area in μm^2. Mean ± s.e.m of n=6.

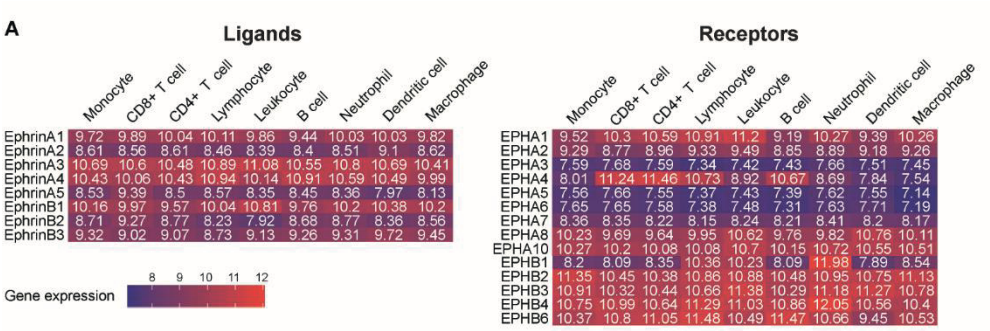
A
Ligands
Monocyte
CD8+ T cell
CD4+ T cell
Lymphocyte
Leukocyte
B cell
Neutrophil
Dendritic cell
Macrophage
EphrinA1 9.72 9.89 10.04 10.11 9.86 9.44 10.03 10.03 9.82
EphrinA2 8.61 8.56 8.61 8.46 8.39 8.4 8.51 9.1 8.62
EphrinA3 10.69 10.6 10.48 10.89 11.08 10.55 10.8 10.69 10.41
EphrinA4 10.43 10.06 10.43 10.94 10.14 10.91 10.59 10.49 9.99
EphrinA5 8.53 9.39 8.5 8.57 8.35 8.45 8.36 7.97 8.13
EphrinB1 10.16 9.97 9.57 10.04 10.81 9.76 10.2 10.38 10.2
EphrinB2 8.71 9.27 8.77 8.23 7.92 8.68 8.77 8.36 8.56
EphrinB3 9.32 9.02 9.07 8.73 9.13 9.26 9.31 9.72 9.45
Gene expression
8 9 10 11 12
Receptors
Monocyte
CD8+ T cell
CD4+ T cell
Lymphocyte
Leukocyte
B cell
Neutrophil
Dendritic cell
Macrophage
EPHA1 9.52 10.3 10.59 10.91 11.2 9.19 10.27 9.39 10.26
EPHA2 9.29 8.77 8.96 9.33 9.49 8.85 8.89 9.18 9.26
EPHA3 7.59 7.68 7.59 7.34 7.42 7.43 7.66 7.51 7.45
EPHA4 8.01 11.24 11.46 10.73 8.92 10.67 8.69 7.84 7.54
EPHA5 7.56 7.66 7.55 7.37 7.43 7.39 7.62 7.55 7.14
EPHA6 7.65 7.65 7.58 7.38 7.48 7.31 7.63 7.71 7.19
EPHA7 8.36 8.35 8.22 8.15 8.24 8.21 8.41 8.2 8.17
EPHA8 10.23 9.69 9.64 9.95 10.62 9.76 9.82 10.76 10.11
EPHA10 10.27 10.2 10.08 10.08 10.7 10.15 10.72 10.55 10.51
EPHB1 8.2 8.09 8.35 10.36 10.23 8.09 11.98 7.89 8.54
EPHB2 11.35 10.45 10.38 10.86 10.88 10.48 10.95 10.75 11.13
EPHB3 10.91 10.32 10.44 10.66 11.38 10.29 11.18 11.27 10.78
EPHB4 10.75 10.99 10.64 11.29 11.03 10.86 12.05 10.56 10.4
EPHB6 10.37 10.8 11.05 11.48 10.49 11.47 10.66 9.45 10.53

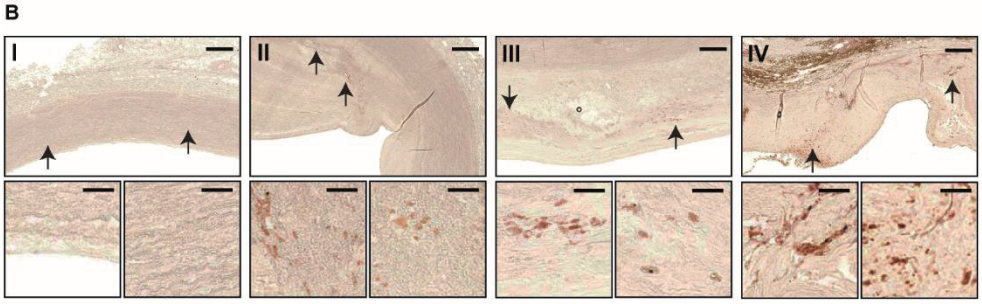
B
I
II
III
IV

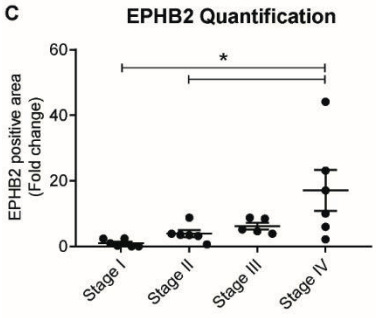
C
EPHB2 Quantification
EPHB2 positive area (Fold change)
60
40
20
0
*
Stage I
Stage II
Stage III
Stage IV

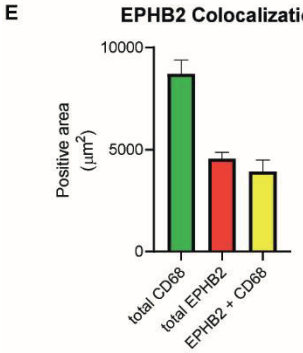
E
EPHB2 Colocalization
Positive area (μm²)
10000
5000
0
total CD68
total EPHB2
EPHB2 + CD68

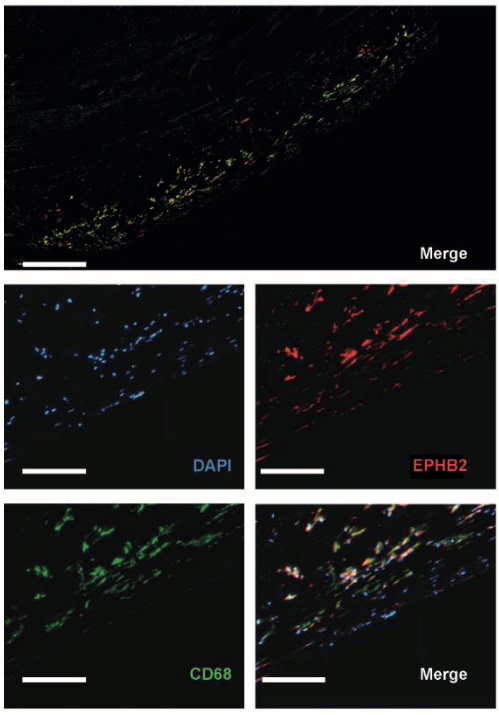
D
Merge
DAPI
EPHB2
CD68
Merge

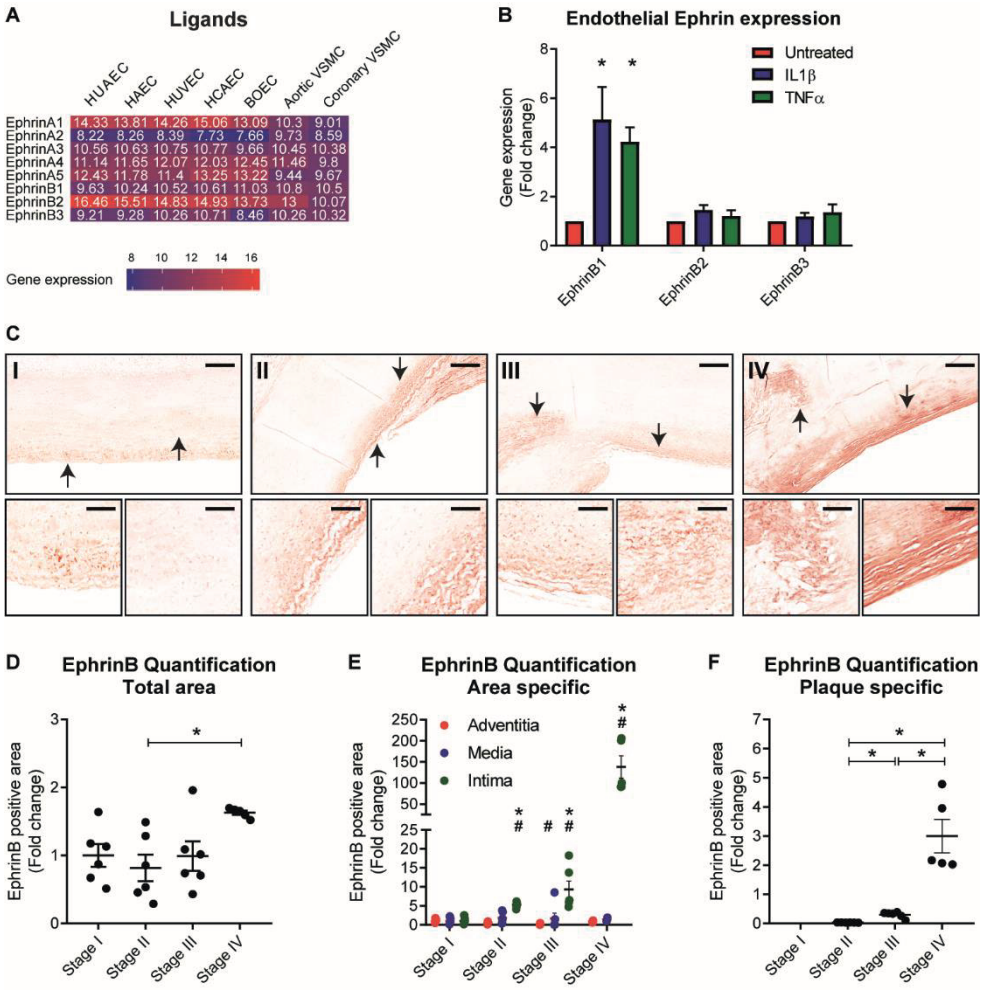

Figure 2 Increased expression of EphrinB in progressive human atherosclerotic lesions. (A) Expression heatmap of Ephrin family ligands in endothelial cells and vascular smooth muscle cells. Blue indicates lower and red higher expression. (B) EphrinB1/B2/B3 expression in HUVECs stimulated with 20 ng/ml IL1β or 10 ng/ml TNFα for 24 hours. Results are relative to untreated cells, set as 1. Mean ± s.e.m. of n=3. *P < 0.05. (C) Overview pictures of immunohistochemical staining for EphrinB in human aortic sections in different stages of atherosclerosis. Lower images show higher-power magnification of the arrow-indicated fields. Scale bars represent 350 and 50 μm respectively. (D-F) Quantification of EphrinB signal on (D) total area, (E) adventitia, media and intima regions and (F) total plaque area. Results are relative to stage I, set as 1. Mean ± s.e.m. of n=6. (D/F) *P<0.05 compared to indicated stages. (E) *P<0.05 representing inter-stage variability within a region compared to stage I and #P<0.05 representing intra-stage variability between regions. (C-F) Stage *I*; Normal, Adaptive Intimal Thickening, Intima Xantoma, *II*; Pathologic Intimal Thickening, Early Fibroatheroma, *III*; Late fibroatheroma, Thin Cap Fibroatheroma, Ruptured Plaque, *IV*; Healing Rupture, Fibrous Calcifies Plaque.

3.2 EPHB2 induced reverse signaling has no effect on endothelial barrier function

Based on the increased EphrinB expression in atherosclerotic plaques and in endothelial cells upon exposure to pro-inflammatory cytokines (Fig. 2), we hypothesized that monocyte binding to the endothelium induces EphrinB reverse signaling, resulting in an altered endothelial barrier function. To investigate the role of potential reverse EphrinB signaling in endothelial cells, we added recombinant EPHB2 protein to endothelial cells and assessed the endothelial barrier function by measuring electrical resistance with ECIS (Fig. 3A). No difference in barrier function of the endothelial monolayer was observed when EphrinB reverse signaling was induced by addition of EPHB2 (Fig. 3B). Higher or lower concentrations of EPHB2 also did not alter barrier function (Supplemental Fig. 3A), while induction of Semaphorin3A signaling did result in a decrease in barrier function (Fig. 3B).

3.3 EphrinB induced forward signaling has no influence on monocyte trafficking

In addition to the role of reverse signaling on endothelial barrier function we assessed the role of EphrinB1 and EphrinB2 induced forward signaling on monocyte adhesion and migration. Monocytes were stimulated with recombinant EphrinB1 or EphrinB2 for 30 minutes before adding them to a confluent monolayer of endothelial cells (Fig. 3C). Both EphrinB1 and EphrinB2 stimulation did not change the adhesion ability of the monocytes, while stimulation with Interleukin 1β (IL1β) did induce monocyte adhesion (Fig. 3D and Supplemental fig. 3B). Next, using the Boyden chamber assay (Fig. 3E), monocyte migration towards MCP-1 in the presence or absence of EphrinB1 or EphrinB2 was examined. We observed that both EphrinB1 and EphrinB2 in the absence of MCP-1 had no chemoattractant effect on the monocytes, nor did EphrinB1 or EphrinB2 in combination with MCP-1 had an antagonistic effect on monocyte chemotaxis (Fig. 3F).

3.4 EPHB2 on monocytes promotes monocyte adhesion and migration

As an ligand-dependent effect for EPHB2 could not be confirmed, we tested the ligand-independent potential of EPHB2 on monocyte adhesion and migration. For this, EPHB2 expression in THP1 cells was silenced using a lentiviral shRNA targeting *EPHB2* mRNA. A non-*EPHB2* targeting scrambled shRNA was used as a control. Repression of EPHB2 was validated using qPCR and immunoblot, showing a decrease by approximately 75% on mRNA level and 40% on protein level (Fig. 4A-C). Adhesion of these THP1 cells to either fibronectin or to a confluent monolayer of HUVECs was diminished compared to control THP1 cells (Fig. 4D-F). Stimulation of THP1 cells with EphrinB1 or EphrinB2 before adhesion to HUVECs did not result in differences in adhesion capacity of the EPHB2 knockdown THP1 cells (Fig. 4F and Supplemental fig. 3B). In line with the

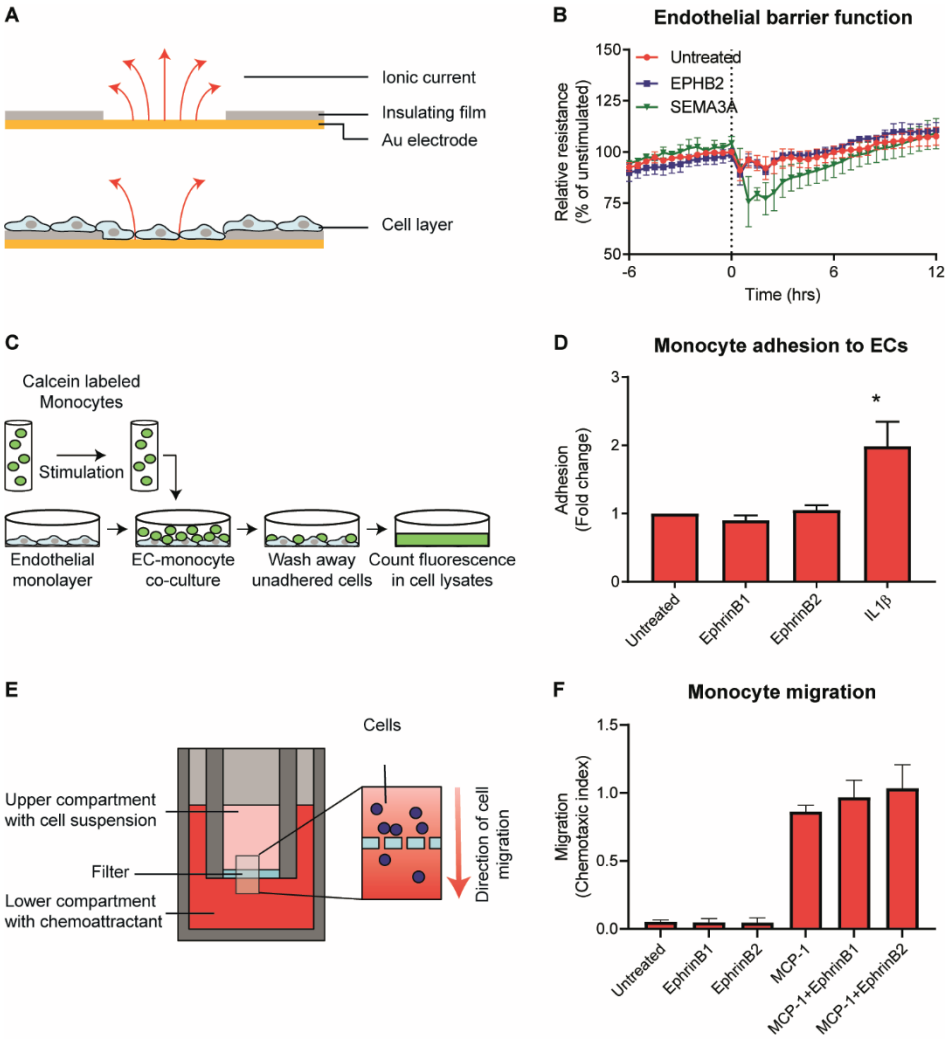

Figure 3 Induced EPH-Ephrin signaling has no effect on endothelial barrier function, monocyte migration and adhesion. (A) Schematic overview of the ECIS system, where changes in resistance by e.g. adherent cells are measured. (B) Transendothelial electrical resistance of HUVECs cultured on ECIS electrodes treated with EPHB2, SEMA3A (positive control) or vehicle (untreated) at t=0. Barrier function is represented as percentage resistance of unstimulated HUVECs at time point 0. Mean ± s.e.m. of n=3. (C) Schematic overview of the adhesion assay. (D) Quantification of adhesion of unstimulated THP1 cells, THP1 cells stimulated with recombinant EphrinB1/B2 (500 ng/ml) or the positive control IL1β (20 ng/ml). Results are presented relative to unstimulated cells, set as 1. Mean ± s.e.m. of n=3. *P<0.05. (E) Schematic overview of the Boyden chamber assay. (F) Quantification of migration of THP1 cells towards MCP-1 (10 ng/ml) alone or combined with EphrinB1/B2. Data is presented as relative to unexposed cells, set as 1. Mean ± s.e.m. of n=3.

reduced adhesion of EPHB2 knockdown THP1 cells, also migration towards MCP-1 was decreased in the EPHB2 knockdown THP1 cells compared to control cells, which was not influenced by the addition of EphrinB1 or EphrinB2 (Fig. 4G).

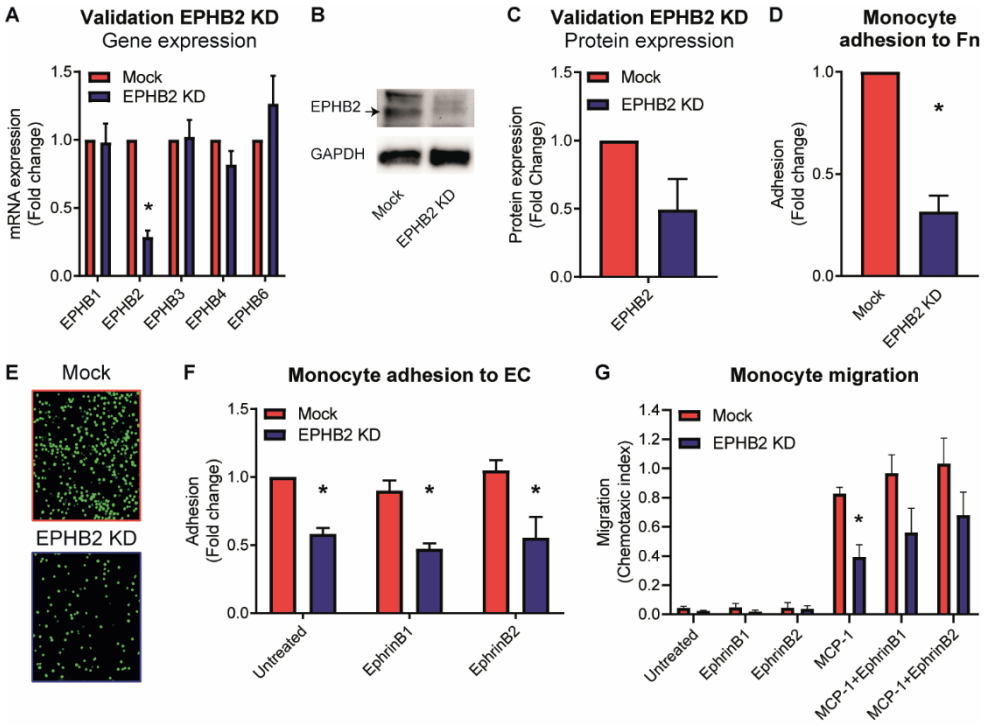

Figure 4 Loss of EPHB2 on monocytes reduces monocyte adhesion and migration. (A) mRNA expression of EPHB1/B2/B3/B4/B6 in mock control monocytes or monocytes treated with a shRNA against EPHB2. Results are relative to mock control cells, set as 1. Mean ± s.e.m. of n=3. *P < 0.05. (B) Immunoblots and (C) quantification of EPHB2 expression in mock and EPHB2 knockdown THP1 cells. Expression is corrected for GAPDH and expressed as fold change compared to mock THP1 cells, set as 1. Mean ± s.e.m. of n=4. (D-F) Quantification of adhesion of mock and EPHB2 knockdown THP1 cells to (D) fibronectin-coated wells or (E-F), either unstimulated or stimulated with EphrinB1/B2 (500 ng/ml), to HUVECs. Results are relative to untreated control cells, set as 1. Mean ± s.e.m. of n=15 or n=3 respectively. *P < 0.05. (G) Migration of mock cells and EPHB2 knockdown THP1 cells to MCP-1 (10 ng/ml) alone or combined with EphrinB1/B2. Data is presented as relative to unexposed cells, set as 1. Mean ± s.e.m of n=3.

3.5 EPHB2 affects actin cytoskeleton via phosphorylation of FAK

To explain the reduced adhesion and migration of THP1 cells with reduced levels of EPHB2 we hypothesize that this could be mediated by changes in the expression levels of the MCP-1 receptor C-C chemokine receptor 2 (CCR2) or the main binding integrin of monocytes Integrinβ-1 (ITGB1). mRNA expression of *CCR2* did not differ in EPHB2

knockdown cells compared to mock treated cells while mRNA levels of *ITGB1* were slightly, but significantly decreased (Fig. 5A). Despite the observed moderate decrease in *ITGB1* on mRNA level, no change was observed in protein expression of ITGB1 (Fig. 5B). Visualization of the cells revealed a more rounded morphology and smaller cell area upon adhesion in monocytes with reduced expression of EPHB2 compared to control monocytes (Fig. 5C and D). Based on this observation polarization of the monocytes was evaluated by determining expression levels of the inflammatory macrophage (M1) markers tumor necrosis factor α (TNFα), IL1β, IL6 and CD86 and the anti-inflammatory macrophage (M2) markers IL10 and CD163 in monocytes and monocyte-derived macrophages with or without a knockdown of EPHB2. While differences in marker expression were observed between monocytes and macrophages, no clear differences in expression between mock control and EPHB2 knockdown cells were observed (Supplemental figure 4A and B). Next, cellular pathways involved in regulation of the cytoskeleton, such as phosphorylation of the mitogen-activated protein kinase (MAPK) pathway (p42-44 and p38), protein kinase B (AKT) and Focal Adhesion Kinases (FAK) were evaluated. While phosphorylation of p42-44, p38 and AKT were comparable between EPHB2 knockdown and mock control cells, we observed a significant decrease in phosphorylation of FAK at Y397 in EPHB2 knockdown cells. Phosphorylation of FAK at Y925 was also lower in EPHB2 knockdown cells, but this difference did not reach statistical significance (Fig. 5E and F). We next investigated whether phosphorylation of FAK via EPHB2 was entirely ligand-independent and not caused by a *cis* interaction between the EPHB2 receptor and its EphrinB ligands on the same cell. From the EphrinB ligands, monocytes highly expressed EphrinB1 (Fig. 1A). We therefore transduced THP1 cells with a lentiviral shRNA targeting EphrinB1 mRNA. Gene and protein analysis showed a significant reduction in EphrinB1 expression and a slight reduction of EphrinB2 (Supplemental Fig. 5A-C). In these cells we observed an increase in phosphorylation of FAK upon knockdown of EphrinB ligands compared to control cells (Fig. 5G and H). Together with the reduced FAK phosphorylation upon EPHB2 knockdown, this suggests that activation of FAK via EPHB2 most likely occurs via receptor dimerization and is independent of its ligand in both *cis* and *trans* interactions (Fig. 5I).

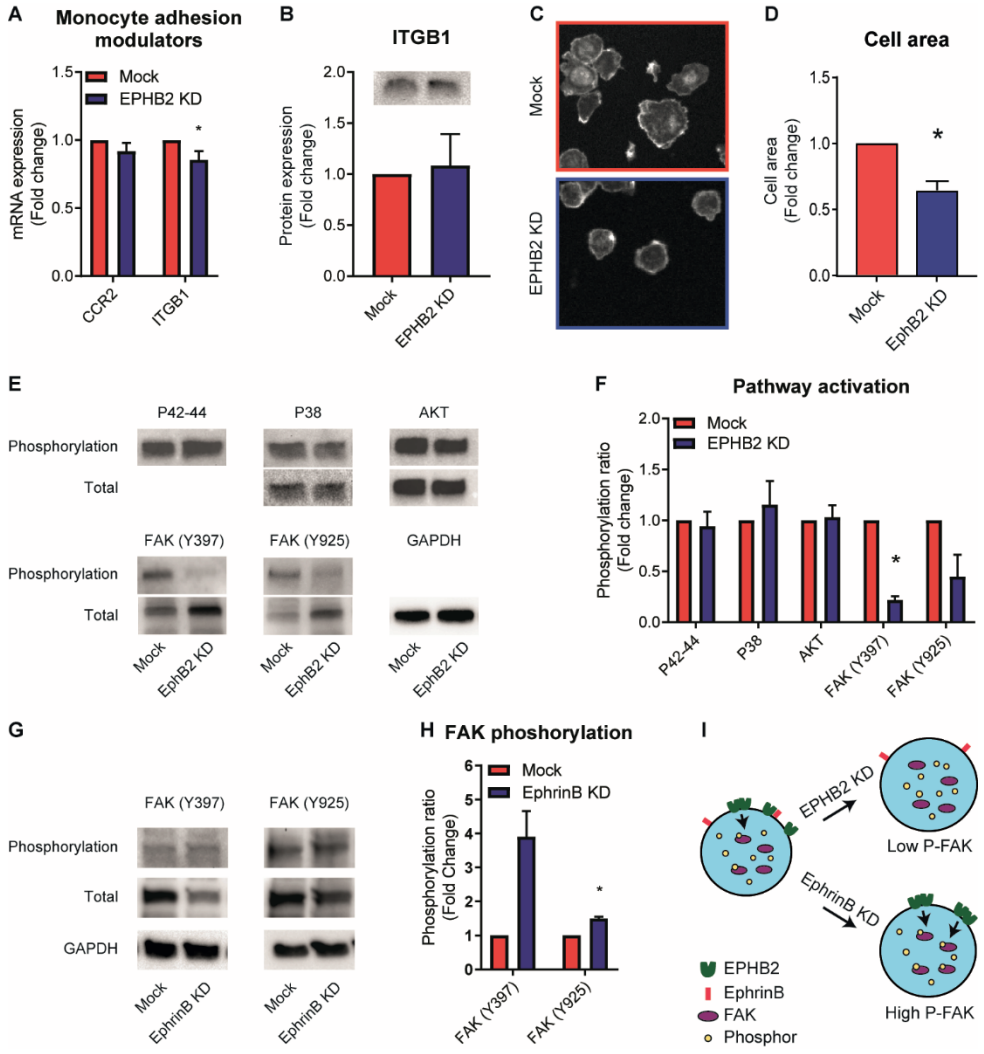

Figure 5 Reduced cell spreading and decreased phosphorylation of FAK in THP1 cells with decreased expression of EPHB2. (A) *CCR2* and *ITGB1* expression in control and EPHB2 knockdown monocytes. Results are relative to mock control cells, set as 1. Mean ± s.e.m. of n=3. *P < 0.05. (B) Quantification of ITGB1 immunoblot expressed as fold change compared to control THP1 cells and corrected for GAPDH. (C) Representative pictures and (D) quantification of the cell surface area of adhered control and EPHB2 knockdown THP1 cells. Results are relative to mock control cells, set as 1. Mean ± s.e.m. of n=3. *P < 0.05. (E) Immunoblots and (F) quantification of phospho- and total P38, P42-44, AKT, FAK (Y397 and Y925) and GAPDH in control cells and EPHB2 knockdown cells. (G) Immunoblots and (H) quantification of phospho- and total FAK (Y397 and Y925) and GAPDH in control cells and EphrinB knockdown cells. (G-H) Expression is expressed as fold change compared to mock THP1 cells and is corrected for total protein expression. Mean ± s.e.m. of n=3. *P < 0.05. (I) Schematic diagram of the effect of EPHB2 and EphrinB expression on FAK phosphorylation in monocytes.

4. Discussion

It is acknowledged that Ephrin family members are involved in atherosclerotic related processes, like amongst others leukocyte chemotaxis, adhesion and migration and regulation of atherosclerotic inflammation (12-14, 24). This is not surprising since EPHA2, EPHA8 and EPHB2, are located within the murine Athsq1 atherosclerosis susceptibility locus (25), which is highly homologous to the premature myocardial infarction susceptibility locus in human (18) that similarly contains EPHA2, EPHA8 and EPHB2. Using multiple functional assays we now show pro-atherosclerotic functions of EPHB2, since reduced levels of this receptor resulted in less monocyte adhesion and migration via decreased phosphorylation of FAK, suggesting a role for EPHB2 in monocyte accumulation in atherogenesis.

In the current study we have shown, for the first time to our knowledge, a plaque burden-dependent expression of EPHB2 and EphrinB ligands in atherosclerotic plaques. In accordance to a paper of Sakamoto and coworkers we show that expression of EPHB2 and EphrinB is increased in advanced atherosclerotic plaques (14), but we now add that expression of EPHB2 proportionally increases with plaque burden. Most of the EPHB2 was found in cells of the monocyte/macrophage lineage, while an increase in EphrinB ligand was mainly observed in the intima of the vessel wall where also the endothelial cells reside. However, this layer is often disrupted and/or damaged during atherosclerotic plaque progression and we also observed an increase of expression within the plaque area itself, indicating that EphrinB expression is not specific to endothelial cells but also present in other cells, for examples macrophages, smooth muscle cells and T lymphocytes.

Ephrins and their receptors are expressed on both endothelial cells and leukocytes. It is therefore not surprising that they are involved in monocyte-endothelial interactions. Forward and reverse signaling of the monocytic EPHB receptors and endothelial EphrinB ligands are on one end proposed to stimulate monocyte adhesion and transmigration, while on the other end to reduce the barrier of endothelial monolayers (26-28). Despite the increase of both EPHB2 and EphrinB ligands in plaque tissue we were not able to delineate the exact role for this receptor-ligand combination in the monocyte-endothelial interactions important for atherogenesis in our in vitro experiments. Not only did activation of endothelial EphrinB ligands, by exposing them to recombinant EPHB2 receptor, have no effect on endothelial barrier function but also activation of EPH receptors on monocytes with recombinant EphrinB ligands had no effect on monocyte adhesion and little effect on migration. While our results seem to be in difference with other studies that have shown that both EphrinB1 and EPHB2 can inhibit the migration of monocytes (14), it should be noted that the means of Ephrin

ligand presentation is of importance. While a surface coated with Ephrin ligands repels leukocyte migration (14, 29), soluble EphrinB ligand in a Transwell system promotes migration of primary blood mononuclear cells (10, 30). Our study adds that EphrinB1/B2 present in the lower compartment of a Transwell system had no chemo-attractive effect on THP1 monocytes and that stimulation with soluble EphrinB1 or EphrinB2, did not influence the adhesion capacity of monocytes.

However, our in vitro data did show that knockdown of EPHB2 in monocytes resulted in impaired adhesion and migration of these monocytes compared to control monocytes. Again, the presence of either EphrinB1 or EphrinB2 did not change monocyte adhesion and slightly increased monocyte migration but this effect was independent of the presence of the EPHB2 receptor on monocytes. Since EphrinB1 and EphrinB2 do not solely bind to EPHB2 (7), other receptor-ligand interactions may have resulted in this effect. Taken together, these results suggest a ligand-independent function of EPHB2 in monocyte adhesion and migration.

The actin cytoskeleton is known to be important for monocyte cellular shape and can thereby influence monocyte adhesion and migration. We indeed observed that EPHB2 knockdown monocytes adopt a specific and rounded shape preventing cellular adhesion and cell spreading. It is known that FAKs are important regulators in cell remodeling and cell migration. Phosphorylation of FAK at Tyr397 (Y397) results in binding and activation of Src protein tyrosine kinases, which then can activate for example small GTPases, and thereby regulate the cells actin cytoskeleton and cellular migration. Earlier studies have already implicated a role for EPH-Ephrin signaling, mainly EPHA2, and focal adhesion kinases in regulation of the actin cytoskeleton (31, 32). Moreover, Batlle et al. showed in colon epithelial tumor cells that stimulation with EphrinB1 results in reduced FAK activation (33). In our study we have shown that monocytes with diminished EPHB2 expression have less phosphorylation of FAK Tyr397 explaining the reduced cell spreading, adhesion and migration capacity of these cells. No significant changes were observed in the FAK phosphorylation at Tyr925 (Y925), which is in line with unchanged MAPK phosphorylation as FAK phosphorylation at Tyr925 is linked to the activation of the extracellular signal regulated MAPK pathway (34). Due to the complex nature of EPH receptor interactions, it is not surprising that EPH receptors can function independent of its ligand. Earlier studies have for example shown that unstimulated EPHA2 receptors are constitutively associated with FAK (35). This was followed by studies of Barquilla et al. and Miao et al. indicating ligand-independent regulation of EPHA2 signaling (36, 37). To complicate it even further, EPH receptors can also signal in a lateral *cis* interaction between EPH receptors and Ephrins on the same cell (38, 39), inducing forward signaling within the same cell. For EPHB2 a

ligand-independent function has not been shown before. As monocytes highly express EphrinB1 and EphrinB1 has a high affinity for the EPHB2 receptor (7) a *cis* interaction in monocytes could occur. However, our result that monocytes with a knockdown in EphrinB ligand do not have a decreased, as would be expected in loss of *cis* interaction-induced signaling, but an increased activity of FAK renders it highly unlikely for an EPHB2-EphrinB *cis* interaction to regulate FAK activity in monocytes. The observed increase in FAK activity upon EphrinB knockdown might be explained by more unbound EPHB2 receptor present on the cell membrane allowing for EPHB2 dimerization and phosphorylation of FAK. Taken together, we propose a mechanism by which EPHB2 on monocytes without ligand, neither in a *trans*- nor a *cis*-interaction, associates with FAK and thereby promotes Y397 phosphorylation, cellular remodeling and migration. With the knockdown of EPHB2 the constitutive phosphorylation of FAK is no longer present and the monocytes' actin cytoskeleton is deregulated inhibiting its migration.

As mentioned before, limited in vivo data on the role of EPHB2 in atherosclerosis is available. EPHB2 expression in vivo is not limited to monocytes and is expressed in a broad range of other cell types including e.g. neurons, T-cells and intestinal (progenitor) cells (16). In line with the variety of cells that express EPHB2, there is also a wide range of functions known for EPHB2 ranging from axonal and vascular patterning during development (40) to e.g. regulating cellular invasiveness of cancer cells (41). So even though general EPHB2 knockout mice are viable and available, research seems to be holding back because of the broad range of potent and essential biological functions of Ephrins during development and in (pathological) physiology. However, specific knockout of EPHB2 in the monocytic cell lineage would be an interesting way to further study the role of monocytic EPHB2 in atherosclerosis in vivo.

In line with the limited amount of in vivo studies, to date also no clinical studies have been conducted on the potential therapeutic options of EPHB2 and its EphrinB ligands in inflammation, immunity or atherosclerosis. In cancer research several clinical trials are conducted with different EPH receptor targeting agents (42), but for EPHB2, clinical trials are still awaiting. Despite some promising results with a drug-conjugated antibody raised against EPHB2, which is expressed in melanoma's, neuroblastomas, gastric, lung and colon cancers (43-46), which could induce cell death in EPHB2 expressing cells both in vitro and in vivo (47), no clinical data has been reported yet. Whether this antibody will be a useful treatment option needs to be further investigated and discovering its therapeutic potential might even guide the way for its implication in other diseases like e.g. atherosclerosis.

Since we have shown in this study that lowering the expression of EPHB2 on monocytes inhibits monocyte adhesion and migration, cell specific targeting of EPHB2

remains a promising potential therapeutic target for atherosclerotic disease. The upcoming field of antisense oligonucleotides (ASOs) (48) might in time provide opportunities to specifically deliver ASOs raised against EPHB2 to inflamed regions and thereby reduce subendothelial monocyte accumulation. However, these options are still far from clinically relevant and further exploration of not only the ASOs but also EphrinB and EPHB2 is essential for discovering new therapeutic options.

In summary, the present study demonstrates an increased expression of EphrinB and EPHB2 in progressive human atherosclerotic tissue. Although the exact means by which Ephrins affect atherosclerosis development remains to be elucidated, we have shown that EPHB2 plays a role in atherosclerosis by mechanisms that are not related to the activation by *trans* nor *cis* interaction of the currently known EphrinB ligands. We show that the effect of EPHB2 is partially explained by its effect on FAK phosphorylation. The EPHB2 receptor-induced increase in FAK phosphorylation results in a cytoskeletal rearrangement, rendering the monocytes more prone to adhere, spread and migrate through the endothelial cell layer, which could contribute to monocyte/macrophage accumulation and progression of atherosclerosis.

Authorship

DV and CB contributed equally to the manuscript. DV, CB, HZ, KH, AvZ and JvG conceptualized and designed the study and contributed to analysis and interpretation. DV, CB, SC, RL, AK and JvG performed the data collection. DV and CB drafted the paper. GKH and JvG revised the work and approved the final version of the manuscript.

Acknowledgments and funding

We would like to say special thanks to dr. J. H. Lindeman from the biobank of Leiden University for the provision of the coupes with atherosclerosis. We also thank Chantal Kroone in providing reagents at very short notice. This research was supported by a grant from the Dutch Heart Foundation (2013T127 to HZ and JvG), by the Rembrandt Institute for Cardiovascular Science (to CB and DV, 2015), in part by a grant to JvG from European Research Area Network on Cardiovascular Diseases (038 MISsCVD), in part by a grant to AvZ from the Dutch Heart Foundation (CVON RECONNECT) and by a VIDI grant (016.156.445) received by GKH from the Dutch Science Organisation. We are also grateful to all our colleagues from the Amsterdam UMC and the Leiden UMC for their comments, insights and support during the experimental phase and during the process of writing this paper.

Conflict of interest

GKH has served as consultant and speaker for biotech and pharmaceutical companies that develop molecules that influence lipoprotein metabolism, including Regeneron, Pfizer, MSD, Sanofi and Amgen. Until April 2019 Hovingh has served as PI for clinical trials conducted with a.o. Amgen, Sanofi, Eli Lilly, Novartis, Kowa, Genzyme, Cerenis, Pfizer, Dezima, Astra Zeneca. The department of vascular medicine receives the honoraria and investigator fees for sponsor studies/lectures for companies with approved lipid lowering therapy in the Netherlands. Since April 2019 Hovingh is partly employed by Novo Nordisk (0.7FTE) and the AMC (0.3FTE). Hovingh has no active patents nor share or ownership of listed companies.

The other authors declare that the research was conducted in the absence of any commercial or financial relationships that could be construed as a potential conflict of interest.

References

1. Nichols M, Townsend N, Scarborough P, Rayner M. Cardiovascular disease in Europe 2014: epidemiological update. Eur Heart J. 2014;35(42):2929. doi: 10.1093/eurheartj/ehu378. PubMed PMID: 25381246.
2. Benjamin EJ, Blaha MJ, Chiuve SE, Cushman M, Das SR, Deo R, et al. Heart Disease and Stroke Statistics-2017 Update: A Report From the American Heart Association. Circulation. 2017;135(10):e146-e603. doi: 10.1161/CIR.0000000000000485. PubMed PMID: 28122885; PubMed Central PMCID: PMCPMC5408160.
3. Sabatine MS, Giugliano RP, Pedersen TR. Evolocumab in Patients with Cardiovascular Disease. N Engl J Med. 2017;377(8):787-8. doi: 10.1056/NEJMc1708587. PubMed PMID: 28834471.
4. Verweij SL, Duivenvoorden R, Stiekema LCA, Nurmohamed NS, van der Valk FM, Versloot M, et al. CCR2 expression on circulating monocytes is associated with arterial wall inflammation assessed by 18F-FDG PET/CT in patients at risk for cardiovascular disease. Cardiovascular research. 2018;114(3):468-75. Epub 2017/12/01. doi: 10.1093/cvr/cvx224. PubMed PMID: 29186373.
5. Geovanini GR, Libby P. Atherosclerosis and inflammation: overview and updates. Clinical science (London, England : 1979). 2018;132(12):1243-52. Epub 2018/06/23. doi: 10.1042/cs20180306. PubMed PMID: 29930142.
6. Ridker PM, Everett BM, Thuren T, MacFadyen JG, Chang WH, Ballantyne C, et al. Antiinflammatory Therapy with Canakinumab for Atherosclerotic Disease. N Engl J Med. 2017;377(12):1119-31. Epub 2017/08/29. doi: 10.1056/NEJMoa1707914. PubMed PMID: 28845751.
7. Funk SD, Orr AW. Ephs and ephrins resurface in inflammation, immunity, and atherosclerosis. Pharmacological research. 2013;67(1):42-52. Epub 2012/10/27. doi: 10.1016/j.phrs.2012.10.008. PubMed PMID: 23098817.
8. Finney AC, Orr AW. Guidance Molecules in Vascular Smooth Muscle. Frontiers in physiology. 2018;9:1311. Epub 2018/10/05. doi: 10.3389/fphys.2018.01311. PubMed PMID: 30283356; PubMed Central PMCID: PMCPMC6157320.

9. Zhang H, Vreeken D, Bruikman CS, van Zonneveld AJ, van Gils JM. Understanding netrins and semaphorins in mature endothelial cell biology. Pharmacological research. 2018;137:1-10. doi: https://doi.org/10.1016/j.phrs.2018.09.015.
10. van Gils JM, Ramkhelawon B, Fernandes L, Stewart MC, Guo L, Seibert T, et al. Endothelial expression of guidance cues in vessel wall homeostasis dysregulation under proatherosclerotic conditions. Arteriosclerosis, thrombosis, and vascular biology. 2013;33(5):911-9. Epub 2013/02/23. doi: 10.1161/atvbaha.112.301155. PubMed PMID: 23430612; PubMed Central PMCID: PMCPMC3647028.
11. Finney AC, Funk SD, Green JM, Yurdagul A, Jr., Rana MA, Pistorius R, et al. EphA2 Expression Regulates Inflammation and Fibroproliferative Remodeling in Atherosclerosis. Circulation. 2017;136(6):566-82. Epub 2017/05/11. doi: 10.1161/CIRCULATIONAHA.116.026644. PubMed PMID: 28487392; PubMed Central PMCID: PMCPMC5548618.
12. Ende G, Poitz DM, Wiedemann E, Augstein A, Friedrichs J, Giebe S, et al. TNF-alpha-mediated adhesion of monocytes to endothelial cells-The role of ephrinA1. Journal of molecular and cellular cardiology. 2014;77:125-35. Epub 2014/12/03. doi: 10.1016/j.yjmcc.2014.10.010. PubMed PMID: 25451169.
13. Jellinghaus S, Poitz DM, Ende G, Augstein A, Weinert S, Stutz B, et al. Ephrin-A1/EphA4-mediated adhesion of monocytes to endothelial cells. Biochimica et biophysica acta. 2013;1833(10):2201-11. Epub 2013/05/28. doi: 10.1016/j.bbamcr.2013.05.017. PubMed PMID: 23707953.
14. Sakamoto A, Ishibashi-Ueda H, Sugamoto Y, Higashikata T, Miyamoto S, Kawashiri MA, et al. Expression and function of ephrin-B1 and its cognate receptor EphB2 in human atherosclerosis: from an aspect of chemotaxis. Clinical science (London, England : 1979). 2008;114(10):643-50. Epub 2007/12/21. doi: 10.1042/cs20070339. PubMed PMID: 18092944.
15. Sakamoto A, Sugamoto Y, Tokunaga Y, Yoshimuta T, Hayashi K, Konno T, et al. Expression profiling of the ephrin (EFN) and Eph receptor (EPH) family of genes in atherosclerosis-related human cells. The Journal of international medical research. 2011;39(2):522-7. Epub 2011/06/16. doi: 10.1177/147323001103900220. PubMed PMID: 21672356.
16. Pasquale EB. Eph-ephrin bidirectional signaling in physiology and disease. Cell. 2008;133(1):38-52. Epub 2008/04/09. doi: 10.1016/j.cell.2008.03.011. PubMed PMID: 18394988.
17. Funk SD, Yurdagul A, Jr., Albert P, Traylor JG, Jr., Jin L, Chen J, et al. EphA2 activation promotes the endothelial cell inflammatory response: a potential role in atherosclerosis. Arteriosclerosis, thrombosis, and vascular biology. 2012;32(3):686-95. Epub 2012/01/17. doi: 10.1161/atvbaha.111.242792. PubMed PMID: 22247258; PubMed Central PMCID: PMCPMC3325141.
18. Wang Q, Rao S, Shen GQ, Li L, Moliterno DJ, Newby LK, et al. Premature myocardial infarction novel susceptibility locus on chromosome 1P34-36 identified by genomewide linkage analysis. Am J Hum Genet. 2004;74(2):262-71. Epub 2004/01/21. doi: 10.1086/381560. PubMed PMID: 14732905; PubMed Central PMCID: PMCPMC1181924.
19. Hruz T, Laule O, Szabo G, Wessendorp F, Bleuler S, Oertle L, et al. Genevestigator v3: a reference expression database for the meta-analysis of transcriptomes. Adv Bioinformatics. 2008;2008:420747. Epub 2008/01/01. doi: 10.1155/2008/420747. PubMed PMID: 19956698; PubMed Central PMCID: PMCPMC2777001.
20. Yahagi K, Kolodgie FD, Otsuka F, Finn AV, Davis HR, Joner M, et al. Pathophysiology of native coronary, vein graft, and in-stent atherosclerosis. Nature reviews Cardiology. 2016;13(2):79-98. Epub 2015/10/28. doi: 10.1038/nrcardio.2015.164. PubMed PMID: 26503410.
21. Ross R. Atherosclerosis — An Inflammatory Disease. New England Journal of Medicine. 1999;340(2):115-26. doi: 10.1056/nejm199901143400207. PubMed PMID: 9887164.
22. Bobryshev YV, Ivanova EA, Chistiakov DA, Nikiforov NG, Orekhov AN. Macrophages and Their Role in Atherosclerosis: Pathophysiology and Transcriptome Analysis. Biomed Res Int. 2016;2016:9582430.

Epub 2016/08/06. doi: 10.1155/2016/9582430. PubMed PMID: 27493969; PubMed Central PMCID: PMCPMC4967433.

23. Himanen JP, Chumley MJ, Lackmann M, Li C, Barton WA, Jeffrey PD, et al. Repelling class discrimination: ephrin-A5 binds to and activates EphB2 receptor signaling. Nature neuroscience. 2004;7(5):501-9. Epub 2004/04/27. doi: 10.1038/nn1237. PubMed PMID: 15107857.
24. Finney AC, Funk SD, Green J, Yurdagul A, Rana MA, Pistorius R, et al. EphA2 Expression Regulates Inflammation and Fibroproliferative Remodeling in Atherosclerosis. Circulation. 2017. Epub 2017/05/11. doi: 10.1161/circulationaha.116.026644. PubMed PMID: 28487392.
25. Welch CL, Bretschger S, Latib N, Bezouevski M, Guo Y, Pleskac N, et al. Localization of atherosclerosis susceptibility loci to chromosomes 4 and 6 using the Ldlr knockout mouse model. Proc Natl Acad Sci U S A. 2001;98(14):7946-51. Epub 2001/07/05. doi: 10.1073/pnas.141239098. PubMed PMID: 11438740; PubMed Central PMCID: PMCPMC35448.
26. Pfaff D, Heroult M, Riedel M, Reiss Y, Kirmse R, Ludwig T, et al. Involvement of endothelial ephrin-B2 in adhesion and transmigration of EphB-receptor-expressing monocytes. Journal of cell science. 2008;121(Pt 22):3842-50. Epub 2008/10/30. doi: 10.1242/jcs.030627. PubMed PMID: 18957513.
27. Liu H, Devraj K, Moller K, Liebner S, Hecker M, Korff T. EphrinB-mediated reverse signalling controls junctional integrity and pro-inflammatory differentiation of endothelial cells. Thrombosis and haemostasis. 2014;112(1):151-63. Epub 2014/02/14. doi: 10.1160/th13-12-1034. PubMed PMID: 24522257.
28. Braun J, Hoffmann SC, Feldner A, Ludwig T, Henning R, Hecker M, et al. Endothelial cell ephrinB2-dependent activation of monocytes in arteriosclerosis. Arteriosclerosis, thrombosis, and vascular biology. 2011;31(2):297-305. Epub 2010/12/04. doi: 10.1161/atvbaha.110.217646. PubMed PMID: 21127290.
29. Sharfe N, Freywald A, Toro A, Dadi H, Roifman C. Ephrin stimulation modulates T cell chemotaxis. European journal of immunology. 2002;32(12):3745-55. Epub 2003/01/09. doi: 10.1002/1521-4141(200212)32:12<3745::aid-immu3745>3.0.co;2-m. PubMed PMID: 12516569.
30. Kitamura T, Kabuyama Y, Kamataki A, Homma MK, Kobayashi H, Aota S, et al. Enhancement of lymphocyte migration and cytokine production by ephrinB1 system in rheumatoid arthritis. American Journal of Physiology - Cell Physiology. 2008;294(1):C189-C96. doi: 10.1152/ajpcell.00314.2007.
31. Woo S, Rowan DJ, Gomez TM. Retinotopic mapping requires focal adhesion kinase-mediated regulation of growth cone adhesion. The Journal of neuroscience : the official journal of the Society for Neuroscience. 2009;29(44):13981-91. Epub 2009/11/06. doi: 10.1523/jneurosci.4028-09.2009. PubMed PMID: 19890008; PubMed Central PMCID: PMCPMC2796108.
32. Krupke OA, Burke RD. Eph-Ephrin signaling and focal adhesion kinase regulate actomyosin-dependent apical constriction of ciliary band cells. Development (Cambridge, England). 2014;141(5):1075-84. Epub 2014/02/20. doi: 10.1242/dev.100123. PubMed PMID: 24550115.
33. Batlle E, Henderson JT, Beghtel H, van den Born MM, Sancho E, Huls G, et al. Beta-catenin and TCF mediate cell positioning in the intestinal epithelium by controlling the expression of EphB/ephrinB. Cell. 2002;111(2):251-63. Epub 2002/11/01. doi: 10.1016/s0092-8674(02)01015-2. PubMed PMID: 12408869.
34. Hauck CR, Hsia DA, Schlaepfer DD. The focal adhesion kinase--a regulator of cell migration and invasion. IUBMB life. 2002;53(2):115-9. Epub 2002/06/07. doi: 10.1080/15216540211470. PubMed PMID: 12049193.
35. Miao H, Li DQ, Mukherjee A, Guo H, Petty A, Cutter J, et al. EphA2 mediates ligand-dependent inhibition and ligand-independent promotion of cell migration and invasion via a reciprocal regulatory loop with Akt. Cancer Cell. 2009;16(1):9-20. Epub 2009/07/04. doi: 10.1016/j.ccr.2009.04.009. PubMed PMID: 19573808; PubMed Central PMCID: PMCPMC2860958.

36. Barquilla A, Lamberto I, Noberini R, Heynen-Genel S, Brill LM, Pasquale EB. Protein kinase A can block EphA2 receptor-mediated cell repulsion by increasing EphA2 S897 phosphorylation. Molecular biology of the cell. 2016;27(17):2757-70. Epub 2016/07/08. doi: 10.1091/mbc.E16-01-0048. PubMed PMID: 27385333; PubMed Central PMCID: PMCPMC5007095.
37. Miao H, Gale NW, Guo H, Qian J, Petty A, Kaspar J, et al. EphA2 promotes infiltrative invasion of glioma stem cells in vivo through cross-talk with Akt and regulates stem cell properties. Oncogene. 2015;34(5):558-67. Epub 2014/02/04. doi: 10.1038/onc.2013.590. PubMed PMID: 24488013; PubMed Central PMCID: PMCPMC4119862.
38. Carvalho RF, Beutler M, Marler KJ, Knoll B, Becker-Barroso E, Heintzmann R, et al. Silencing of EphA3 through a cis interaction with ephrinA5. Nature neuroscience. 2006;9(3):322-30. Epub 2006/02/24. doi: 10.1038/nn1655. PubMed PMID: 16491080.
39. Hornberger MR, Dutting D, Ciossek T, Yamada T, Handwerker C, Lang S, et al. Modulation of EphA receptor function by coexpressed ephrinA ligands on retinal ganglion cell axons. Neuron. 1999;22(4):731-42. Epub 1999/05/07. doi: 10.1016/s0896-6273(00)80732-1. PubMed PMID: 10230793.
40. Adams RH. Vascular patterning by Eph receptor tyrosine kinases and ephrins. Semin Cell Dev Biol. 2002;13(1):55-60. Epub 2002/04/24. doi: 10.1006/scdb.2001.0289. PubMed PMID: 11969371.
41. Nakada M, Niska JA, Tran NL, McDonough WS, Berens ME. EphB2/R-Ras signaling regulates glioma cell adhesion, growth, and invasion. Am J Pathol. 2005;167(2):565-76. Epub 2005/07/29. doi: 10.1016/S0002-9440(10)62998-7. PubMed PMID: 16049340; PubMed Central PMCID: PMCPMC1603577.
42. Boyd AW, Bartlett PF, Lackmann M. Therapeutic targeting of EPH receptors and their ligands. Nat Rev Drug Discov. 2014;13(1):39-62. Epub 2014/01/01. doi: 10.1038/nrd4175. PubMed PMID: 24378802.
43. Liu W, Ahmad SA, Jung YD, Reinmuth N, Fan F, Bucana CD, et al. Coexpression of ephrin-Bs and their receptors in colon carcinoma. Cancer. 2002;94(4):934-9. Epub 2002/03/29. doi: 10.1002/cncr.10122. PubMed PMID: 11920461.
44. Tang XX, Brodeur GM, Campling BG, Ikegaki N. Coexpression of transcripts encoding EPHB receptor protein tyrosine kinases and their ephrin-B ligands in human small cell lung carcinoma. Clin Cancer Res. 1999;5(2):455-60. Epub 1999/02/26. PubMed PMID: 10037197.
45. Tang XX, Evans AE, Zhao H, Cnaan A, Brodeur GM, Ikegaki N. Association among EPHB2, TrkA, and MYCN expression in low-stage neuroblastomas. Med Pediatr Oncol. 2001;36(1):80-2. Epub 2001/07/24. doi: 10.1002/1096-911X(20010101)36:1<80::AID-MPO1019>3.0.CO;2-N. PubMed PMID: 11464911.
46. Vogt T, Stolz W, Welsh J, Jung B, Kerbel RS, Kobayashi H, et al. Overexpression of Lerk-5/Eplg5 messenger RNA: a novel marker for increased tumorigenicity and metastatic potential in human malignant melanomas. Clin Cancer Res. 1998;4(3):791-7. Epub 1998/05/14. PubMed PMID: 9533549.
47. Mao W, Luis E, Ross S, Silva J, Tan C, Crowley C, et al. EphB2 as a therapeutic antibody drug target for the treatment of colorectal cancer. Cancer Res. 2004;64(3):781-8. Epub 2004/02/12. PubMed PMID: 14871799.
48. Miller CM, Harris EN. Antisense Oligonucleotides: Treatment Strategies and Cellular Internalization. RNA Dis. 2016;3(4). Epub 2016/01/01. doi: 10.14800/rd.1393. PubMed PMID: 28374018; PubMed Central PMCID: PMCPMC5376066.

Supplemental data

Supplemental table 1: Primer sequences.

Gene	Forward sequence	Reverse sequence
GAPDH	CCTGCACCACCAACTGCTTA	GGCCATCCACAGTCTTCTGAG
EphrinB1	GAGGCAGACAACACTGTCAAG	AGCTTCAGTAGTAGGACCGTC
EphrinB2	TGTGGGTATAGTACCAGTCTTG	ACTGCTGGGGTGTTTTGATGG
EphrinB3	TCGGCGAATAAGAGGTTCCA	GTCCCCGATCTGAGGGTACA
EPHB1	TACGGCAAGTTCAGTGGCAA	AGGACACAACGAACACGACC
EPHB2	GCTTCGAGGCCGTTGAGAAT	GAAGTGGTCCGGCTGTTGAT
EPHB3	GTCATCGCTATCGTCTGCCT	AAACTCCCGAACAGCCTCATT
EPHB4	CGCACCTACGAAGTGTGTGA	GTCCGCATCGCTCTCATAGTA
EPHB6	CGACCAGACCAATGGGAACA	GGGTGAAGGAGTGGGATTCG
CCR2	CCACATCTCGTTCTCGGTTTATC	CAGGGAGCACCGTAATCATAATC
ICAM-1	GGCCGGCCAGCTTATACAC	TAGACACTTGAGCTCGGGCA
TNFα	CCTCTCTCTAATCAGCCCTCTG	GAGGACCTGGGAGTAGATGAG
IL1β	ATGATGGCTTATTACAGTGGCAA	GTCGGAGATTCGTAGCTGGA
IL6	AAGCCAGAGCTGTGCAGATGAGTA	AACAACAATCTGAGGTGCCCATGC
IL10	GCGCTGTCATCGATTTCTTCC	GTAGATGCCTTTCTCTTGGAGCTTA
CD86	CTGCTCATCTATACACGGTTACC	GGAAACGTCGTACAGTTCTGTG
CD163	TTTGTCAACTTGAGTCCCTTCAC	TCCCGCTACACTTGTTTTCAC

Supplemental figure 1: Increased EPHB2 expression upon monocyte-to-macrophage differentiation.

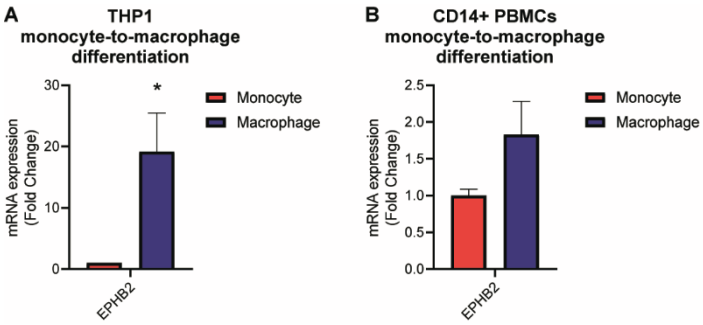

mRNA expression of EPHB2 in monocytes or macrophages derived from (A) THP1 cells or (B) CD14+ derived peripheral blood mononuclear cells. Results are relative to monocytes, set as 1. Mean ± s.e.m. of n=3. *P < 0.05.

Supplemental figure 2: EPHB2 colocalization with CD45.

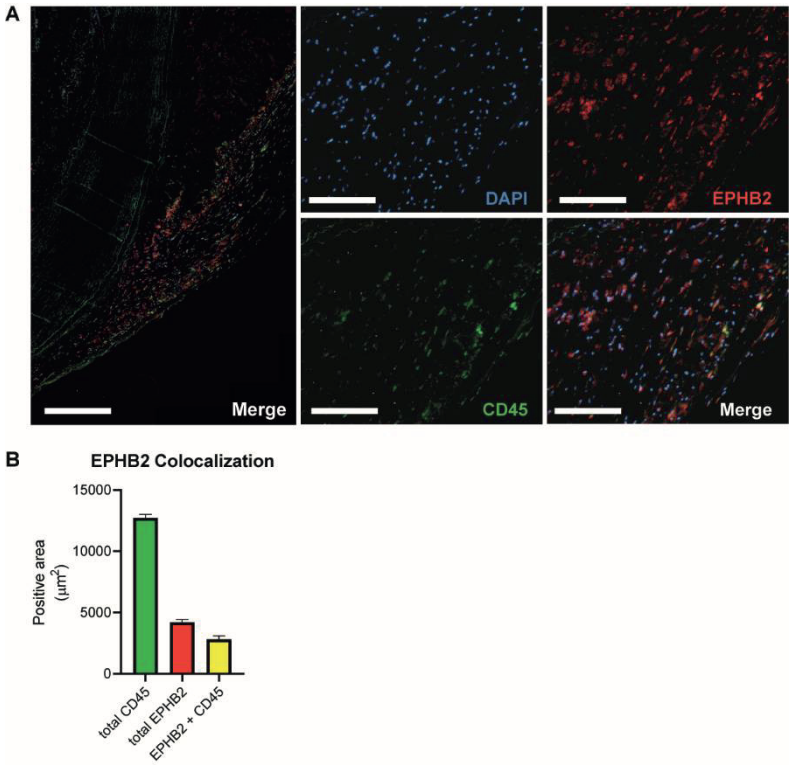

(A) Overview and zoom-in pictures of immunofluorescent staining for EPHB2 (red), CD45 (green) and nuclei (blue) in stage IV human aortic sections. Scale bars represent 300 and 25 µm respectively. (B) Quantification of fluorescent signal in plaque shoulder region. Results are quantified as positive area in µm². Mean ± s.e.m of n=6.

Supplemental figure 3: Different concentrations of recombinant protein did not alter cellular response.

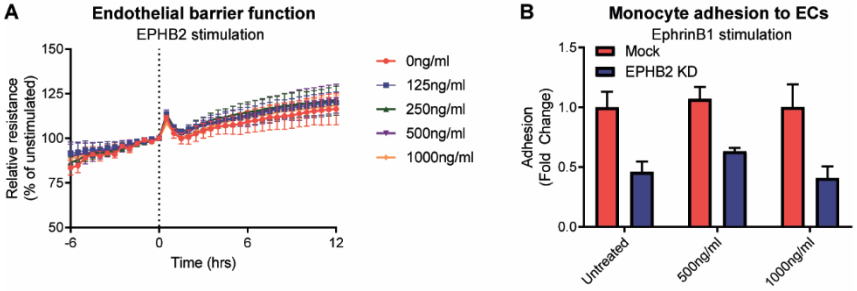

(A) Transendothelial electrical resistance of EPHB2 stimulated HUVECs cultured on ECIS electrodes. Concentrations of EPHB2 ranged from 0 to 1000ng/ml. Barrier function is represented as percentage resistance of unstimulated HUVECs at time point 0. Mean ± s.e.m. of n=3. (B) Adhesion of unstimulated THP1 cells or THP1 cells stimulated with different concentrations of recombinant EphrinB1 (500 or 1000 ng/ml). Results are presented relative to unstimulated cells, set as 1. Mean ± s.e.m. of triplicate samples.

Supplemental figure 4: No altered monocyte/macrophage polarization upon EPHB2 knockdown.

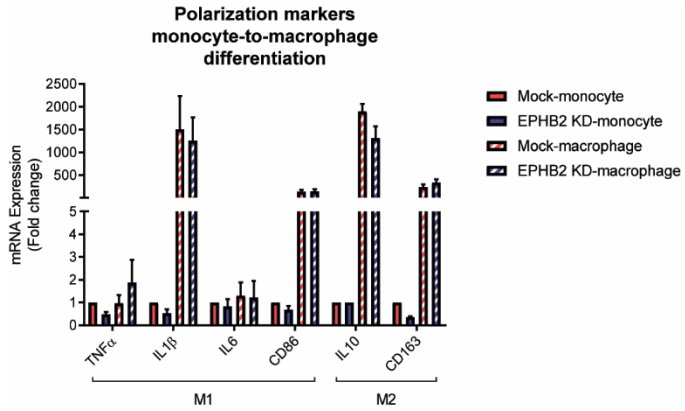

mRNA expression of M1 markers TNFα, IL1β, IL6 and CD86 and M2 markers IL10 and CD163 in monocytes (solid filled bars) or macrophages (striped bars) derived from mock control THP1 cells or THP1 cells with a knockdown in EPHB2. Results are relative to mock control monocytes, set as 1. Mean ± s.e.m. of n = 3.

Supplemental figure 5: Decreased EphrinB expression in shRNA transduced THP1 cells.

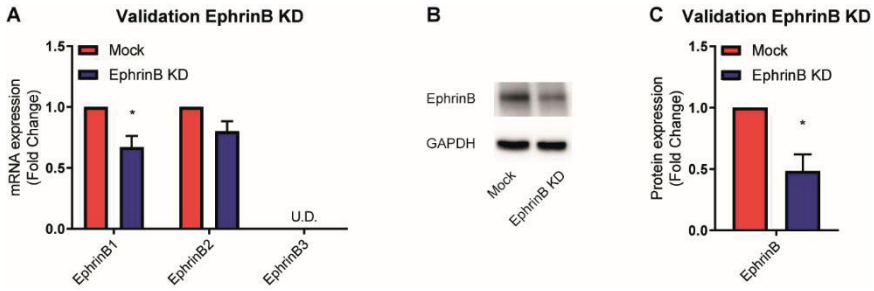

(A) mRNA expression of EphrinB ligands in mock control monocytes or EphrinB knockdown monocytes. Results are relative to mock control cells, set as 1. Mean ± s.e.m. of n=3. *P < 0.05 (B) Immunoblots and (C) quantification of EphrinB expression in mock and EphrinB knockdown THP1 cells. Expression is corrected for GAPDH protein expression and expressed as fold change compared to mock THP1 cells, set as 1. Mean ± s.e.m. of n=3. *P < 0.05.